Revista
GEOCIÊNCIAS

unesp

ISSN: 1980-900X (online)

PALEOPROTEROZOIC GRAPHITIZATION IN THE CLÁUDIO SHEAR ZONE (SOUTHERN SÃO FRANCISCO CRATON - BRAZIL) INVESTIGATED BY RAMAN SPECTROSCOPY AND X-RAY DIFFRACTION

GRAFITIZAÇÃO PALEOPROTEROZOICA NA ZONA DE CISALHAMENTO CLÁUDIO (SUL DO CRÁTON DO SÃO FRANCISCO - BRASIL) INVESTIGADA POR ESPECTROSCOPIA RAMAN E DIFRAÇÃO DE RAIOS X

Raphael Martins COELHO[1], Alexandre de Oliveira CHAVES[1], Sérgio Luís Lima de Moraes RAMOS[2]

[1]Universidade Federal de Minas Gerais, Programa de Pós-graduação em Geologia, Instituto de Geociências, Departamento de Geologia, CPMTC-IGC. Avenida Antônio Carlos 6627, Pampulha - Belo Horizonte, MG – Brasil.
E-mails: raphaelmcoelho@yahoo.com.br; alochaves@yahoo.com.br
[2]Universidade Federal de Minas Gerais Centro de Tecnologia de Nanomateriais (CTNano). Rua Professor José Vieira de Mendonça, 1000 - Engenho Nogueira, Belo Horizonte - MG, Brazil. E-mail: slramos@ctnano.org

ABSTRACT - The southern São Francisco craton hosts some of the largest graphite mines in Brazil, located in the city of Itapecerica. This paper addresses graphite crystals that occur within the regional structure known as the Cláudio shear zone in terms of thermometry. Raman spectroscopy and X-ray diffraction data showed that, on average, graphite crystals of the Cláudio shear zone have high crystallinity and are similar to those from mines in Itapecerica. The average temperature found (702 ºC) in this study is close to the samples from Itapecerica. However, this temperature is still lower than the expected (~900 ºC) from previous studies. The hypothesis for this would be that the graphite devolved high crystallinity, but was modified during the evolution of the metamorphism, or during the post-collisional stage fluid percolation. Thus, the modified crystallinity parameters lead to the relatively low-temperature values found. The proximity and similarity of geological framework suggest correlation between the precursor basins that formed the Itapecerica and the Cláudio shear zone graphite occurrences. From a global perspective, the closure of precursor basins and formation of the Cláudio shear zone are part of the collisions of Archean and Paleoproterozoic crustal blocks that formed the Columbia supercontinent.
Keywords: Graphite. High-grade metamorphism. Raman spectroscopy. Southern São Francisco craton. X-ray diffraction.

RESUMO - O sul do cráton do São Francisco abriga algumas das maiores minas de grafite do Brasil, localizadas na cidade de Itapecerica. Este artigo aborda cristais de grafite que ocorrem dentro da estrutura regional conhecida como zona de cisalhamento de Cláudio em termos de termometria. Dados de espectroscopia Raman e difração de raios X mostraram que, em média, os cristais de grafite da zona de cisalhamento de Cláudio possuem alta cristalinidade e são semelhantes aos das minas de Itapecerica. A temperatura média encontrada (702 ºC) neste estudo está próxima das amostras de Itapecerica. No entanto, esta temperatura ainda está abaixo do esperado (~900 ºC) de estudos anteriores. A hipótese para isso seria que o grafite degenerou alta cristalinidade, mas foi modificado durante a evolução do metamorfismo, ou durante o estágio pós-colisional de percolação do fluido. Assim, os parâmetros de cristalinidade modificados levam aos valores de temperatura relativamente baixos encontrados. A proximidade e similaridade do arcabouço geológico sugerem correlação entre as ocorrências das bacias precursoras que formaram a Itapecerica e a zona de cisalhamento de Cláudio. Do ponto de vista global, o fechamento de bacias precursoras e a formação da zona de cisalhamento Cláudio fazem parte das colisões de blocos crustais do Arqueano e do Paleoproterozoico que formaram o supercontinente Columbia.
Palavras-Chave: Grafita. Metamorfismo de alto grau. Espectroscopia Raman. Sul do cráton do São Francisco. Difração de raios X.

INTRODUCTION

Graphite ordinarily comes from organic matter (derived from the biological activity) that was deposited with sediments, when they subsequently undergo transformations at high temperatures and pressures during metamorphic processes over geological time. The combinations of conditions in the geological environment (pressure, temperature, kinetics, and fluid activity) lead to progressive transformation of disordered or partly ordered non crystalline carbonaceous material (CM) into pure carbon, end-member crystalline graphite. That process is known as graphitization (Buseck & Beyssac, 2014).

According to Crespo et al. (2006), graphite crystallinity can be described both along the stacking direction (c axis) of the carbon layers and along the a-b plane. In the first case, highly crystalline graphite has shorter spacing between adjacent layers of carbon atoms (the d002 spacing from which the c parameter is calculated). In addition, the continuity of the carbon layers along the stacking direction (the Lc crystallite size) is larger than for poorly crystalline graphite. In the second case, crystallinity refers to the continuity of carbon layers along the in-plane directions (defined by the La crystallite size).

The crystallinity, determined by X-ray diffraction (XRD) and Raman spectroscopy, has been used as a geothermometer due to the fact that, in natural environments, crystallinity has been proved to increase (smaller d002, larger Lc and La) with increasing metamorphic grade (Landis, 1971; Grew, 1974; Diessel et al., 1978; Kwiecinska, 1980; Buseck & Bo-Jun, 1985; Tagiri & Oba, 1986; Pasteris & Wopenka, 1991; Wopenka & Pasteris, 1993; Wada et al., 1994; Yui et al., 1996; Nishimura et al., 2000; Beyssac et al., 2002b, 2004; Buseck & Beyssac, 2014; Rantitsch et al., 2016).

Approximately 9 % of graphite production worldwide is mined in Brazil (USGS, 2021), which has several occurrences of graphite generally associated with Paleoproterozoic khondalitic belts (figure 1A). The southern São Francisco craton (SFC) hosts some of the largest Brazilian graphite mines located in the city of Itapecerica (Figure 1A).

The origin and thermometry of the graphite in these mines were previously studied by Miranda et al. (2019). In the vicinity, occurrences of graphite within the regional scale structure known as the Cláudio shear zone (CSZ) have been found, possibly with geological relation to those of the Itapecerica mines (Figure 1B), still have not been studied regarding their origin and thermometry. The objective of this study is to determine, by XRD and Raman spectroscopy, the thermometry of the occurrences close to the city of Cláudio that occur within the CSZ and to compare the obtained results with the graphite data of Miranda et al. (2019) for the Itapecerica mines.

GEOLOGICAL SETTING

The southern sector of São Francisco Craton (Figure 1A) is composed of Meso- to Neoarchaean granite-greenstone terrains, Palaeoproterozoic clastic-chemical metasedimentary rocks (including Itabirites of Quadrilátero Ferrífero (QF)) from Minas Supergroup, and Neoproterozoic pelitic-carbonatic sedimentary rocks from Bambuí Group (Teixeira et al., 2017a).

The Archaean core is composed by the complexes denominated Campo Belo-Bonfim, Divinopolis and Belo Horizonte that are TTG (tonalite-trondhjemite-granodiorite) suites associated to greenstone belts (3.20–2.90 Ga), granitoid plutons generated by partial melting of older material (2.79–2.70 Ga) (Teixeira et al., 2017a), mafic-ultramafic intrusions (Noce et al., 1998), and granitoid rocks emplaced later at 2.61 Ga (Farina et al., 2015). The main supracrustal units of the region are the Neoarchaean greenstone belt sequence (Rio das Velhas Supergroup, 2.77–2.73 Ga) and the Early Palaeoproterozoic Minas Supergroup (Moreira et al., 2016; Teixeira et al., 2017a) (Figure 1B).

The Mineiro Belt (Noce et al., 1998; Ávila et al., 2014; Teixeira et al., 2015) is a large juvenile terrain formed by accretionary orogeny between Siderian and Orosirian periods, which resulted in an extensive reworking of regions placed at the margins of the southern SFC (Noce et al., 2007; Seixas et al., 2013; Teixeira et al., 2015; Barbosa et al., 2019; Moreira et al., 2020 and Lopes et al., 2020). The region is cutted by several generations of mafic dike swarms (Chaves, 2013) from 1.7 Ga (Pará de Minas dike swarm) to 135 Ma (Transminas dyke swarm) (Figure 1B).

A distinct NE-SW trending structure known as Cláudio Shear Zone (CSZ - Figure 1B) is a geological suture that separates the Archean Campo Belo-Bonfim and Divinópolis metamorphic complexes in southern SFC (figure 1B), as evidenced by the high deformation strain with dextral strike-slip motion (Oliveira, 2004; Teixeira et al., 2017b). Metamorphosed ultramafic rocks (metaperidotite, talc-serpentine-chlorite-amphibole schist), amphibolite, garnet-sillimanites schist, graphite schist, quartzite, banded iron formation and sillimanite-cordierite-garnet-biotite gneiss (Oliveira, 2004) outcrop along the CSZ. The foliation within the CSZ mega-structure shows dips from medium to high angle and mylonitic feature in its inner region.

The sillimanite-cordierite-garnet-biotite gneisses, also known as khondalitic paragneisses, are associated with graphite schist, the graphite bearing host rocks in some local graphite mines (Chaves et al., 2015; Teixeira et al., 2017b; Miranda et al., 2019). The khondalitic paragneisses investigated

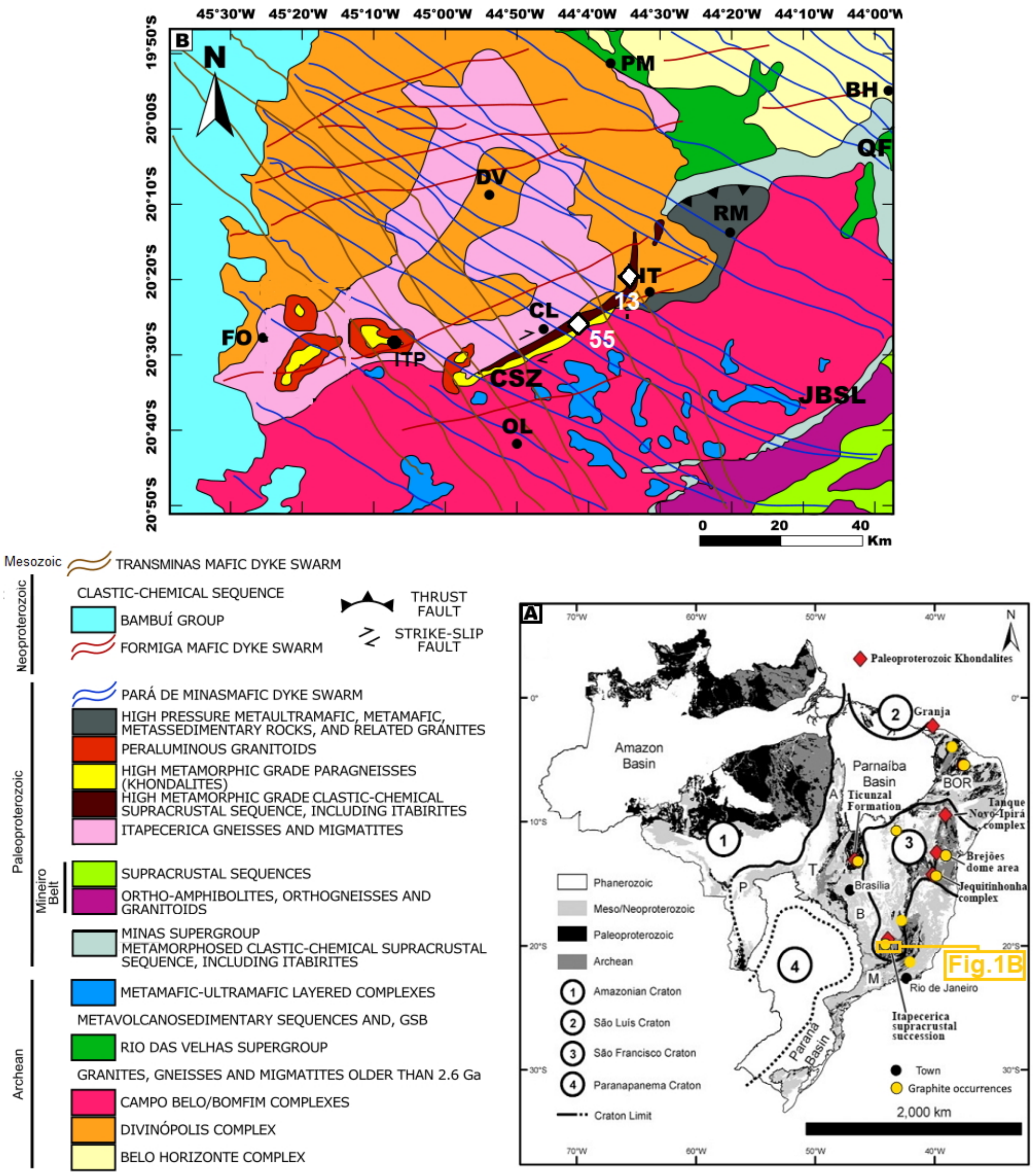

Figure 1 - A – Graphite occurrences in Brazilian shield. BOR – Borborema Structural Province. M – Mantiqueira Structural Province. T – Tocantins Structural Province. P – Paraguai Belt. A – Araguaia Belt. B – Brasília Belt. Modified from Fuck et al. (2014), Klein et al. (2018). B – Geological map of the Southern São Francisco craton, studied area with sampling points as lozenges. QF – Quadrilátero Ferrífero, JBSL – Jeceaba-Bom Sucesso lineament, CSZ – Cláudio shear zone. Cities: BH – Belo Horizonte, PM – Pará de Minas, DV – Divinópolis, RM – Rio Manso, IT – Itaguara, FO – Formiga, CL – Cláudio, OL – Oliveira, ITP – Itapecerica (modified from Chaves et al., 2019).

Coelho & Chaves (2019) indicated metamorphic peak estimate temperatures about 900ºC around 2011 Ma (age determined by chemical U-Th-Pb method in monazites). This age is close to U-Pb zircon ages described by Carvalho et al. (2017) in the Kinawa migmatite (2048 ± 25 and 2034 ± 32 Ma). These ages define a high-grade event in the interior part of the southern SFC Archean core along the CSZ during the granu-lite facies metamorphic peak and confirm the existence of a Paleoproterozoic event previously recognized only from monazite in khondalitic rocks near CSZ (Chaves et al., 2015).

According to Miranda et al. (2019) the town of Itapecerica host the second largest graphite mine in Brazil, located 20 km west of the CSZ. The Itapecerica graphite schist is composed of fine to medium grained graphite, quartz and sillimanite showing granolepidoblastic texture. Graphite is the main component and marks the rock foliation. Quartz is the second main component, with elongated (ribbons) crystals. Sillimanite occurs in variable proportions as fibrous or prismatic habit. The values of δ13C range between -21.23 and -27.89 ‰, indicating that the source of the graphite was a primitive biogenic carbon material. High-grade metamorphic graphite from Itapecerica shows average temperatures around 729 ºC, indicating granulite to amphibolite facies formation conditions.

The graphite occurrences within the CSZ are layers of grayish-colored graphite schist with a few centimeter lengths (Figure 2) surrounded by large hydrothermal quartz veins. The graphite has a very fine grain and the layers rich in quartz generally have boudin- and sigmoid-like structures.

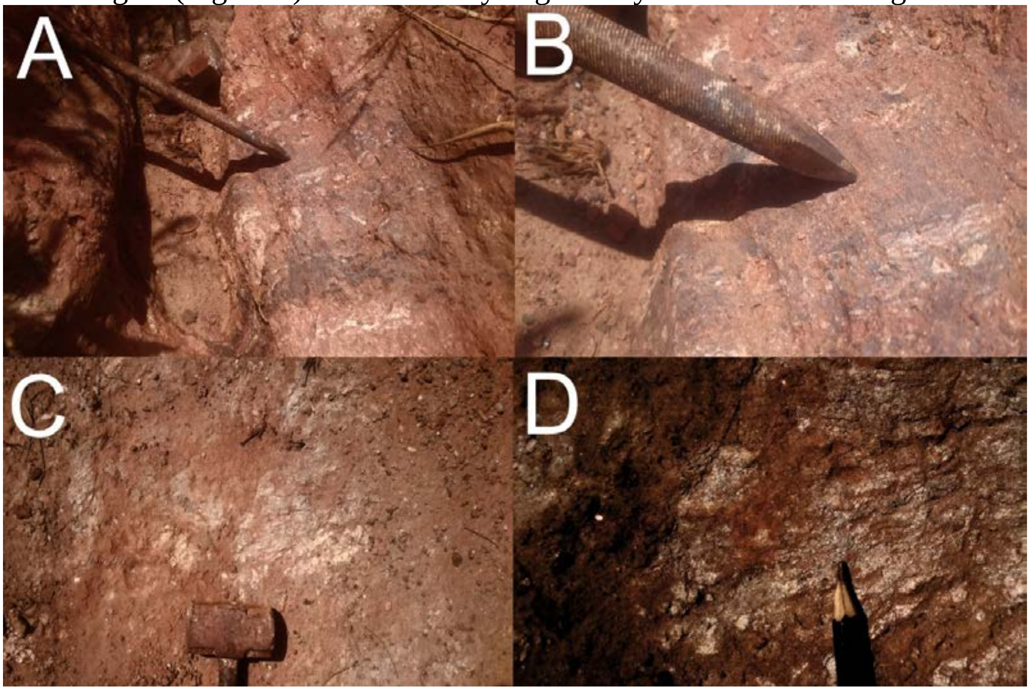

Figure 2 - Graphite schist outcrops from CSZ. A - Sampling point 13; B - Detailed view of the outcrop; C Sampling point 55; D - Detailed view of the outcrop.

The photomicrographs of the graphite schists show that graphite is fine-grained disseminated over the rock, forming aggregates intercalated with layers of quartz and sillimanite (Figure 3), which define the schistosity. The sillimanite crystals are less abundant, often with fibrous habit interspersed with graphite crystals in foliation. The effects of shear stress are well observable above the quartzose layers, such as the dynamic recrystallization of quartz grains, the ribbon quartz, and the anastomosed texture of the quartz layers (Figure 3).

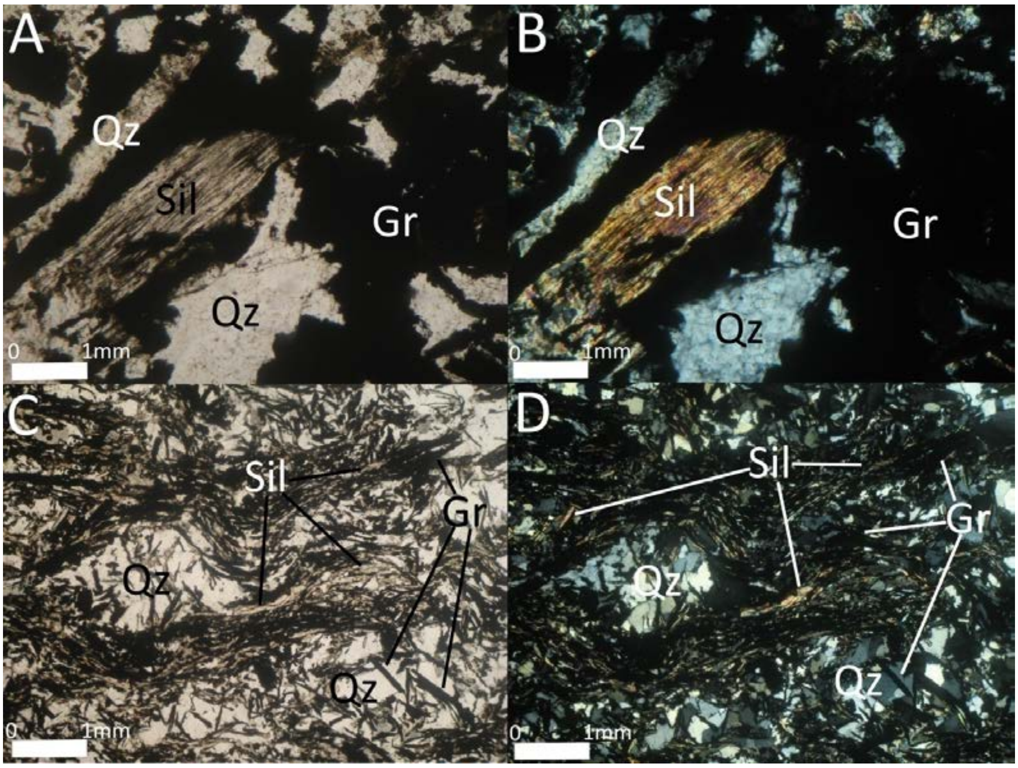

Figure 3 - Photomicrographs illustrating graphite textures: A and B are from sample 13 and C and D from sample 55 showing the scattered aspect of the graphite inside schist (A and C under plane polarized light - PPL and B and D under crossed polarized light-XPL) Mineral abbreviations according to Whitney & Evans (2010): Gr: graphite; Sil: sillimanite; Qz: quartz.

METHODOLOGY AND RESULTS

Two samples of natural graphite from the Cláudio shear zone were collected (sample 13, coordinates 20° 20.480' S 44° 33.469' W; sample 55 coordinates 20° 26.443' S 44° 43.565' W) (sampling location in figure 1B). In Manoel Teixeira da Costa Research Center (CPMTC-IGC-UFMG) laboratories, the graphite schist samples were prepared for the XRD and for Raman spectroscopy. Due to the graphite shists of CSZ being friable, the samples were cautiously disaggregated in an agate mortar to avoid the interference of the grinding for the analysis (Crespo et al., 2006) and subsequently subjected to the flotation process to separate the graphite from the quartz-sillimanite fractions of the rock.

X-Ray Diffraction (XRD)

XRD analyses were performed at the Manoel Teixeira da Costa Research Center (CPMTC-IGC-UFMG, at Belo Horizonte-MG) X-ray Laboratory. XRD spectra were recorded with a PANalytical X´Pert PRO diffraction instrument with theta-theta geometry, using a Cu Kα X-ray source (40 kV and 45 mA). The diffraction data were collected with a step size of 0.02° 2θ and a scan step of 0.5 s.

To obtain lattice parameters of high accuracy, the diffraction data were fitted by Rietveld methods (Young, 1993). The starting parameters for the refinement were identical for each sample and chosen to be as close as possible to realistic values. Based on Tagiri (1981), the standard deviation of the error of d(002) is ~0.02 over 3.53 Å, ~0.01 between 3.53 and 3.36 Å, and ~0.005 between 3.36 and 3.35 Å. The experimental error of Lc(002) is about 4% below 30 Å and about 10% over 500 Å (Tagiri, 1981).

The crystal size (Lc(002)) along stacking direction is estimated from the follow equation (Baiju et al., 2005):

$$Lc(002) = k\lambda/\beta(002)\cos\theta$$

where k is the shape constant (0.9), β(002) is the full width at half maximum of the peak in radian, λ is the X-ray wave length in angstroms (1.5406), and θ is the angle of diffraction in radians.

Further, the graphitization degree (GD) has been calculated from the equation (Tagiri, 1981):

$$GD = \{[d(002) - 3.7]/[Log(Lc(002)/1000)]\} \times 100$$

Additionally, the metamorphism temperature is calculated by the equation for pelitic rocks (Wada et al., 1994):

$$T(°C) = 3.2 \times GD + 280$$

The results are shown in table 1 and graphitization temperatures are between 620 and 781°C.

Table 1 - Graphite XRD diffraction data.

Sample	2θ	$d_{(002)}$ Å	sd ±	FWHM (2θ)	$Lc_{(002)}$ Å	sd ±	GD	T (ºC)	sd ±
13a	26.633	3.347	0.005	0.157	519	52	124	676	34
13b	26.605	3.351	0.005	0.138	592	59	154	772	39
13c	26.498	3.361	0.01	0.144	567	57	138	720	36
13d	26.620	3.346	0.005	0.168	508	51	120	665	33
55a	26.669	3.343	0.005	0.177	461	46	106	620	31
55b	26.656	3.344	0.005	0.138	593	59	157	781	39
55c	26.620	3.346	0.005	0.168	486	49	113	642	32
55d	26.668	3.340	0.005	0.144	567	57	146	747	37

sd: standard deviation.

The binary plot of Lc(002) vs. d(002) (Tagiri & Oba, 1986) shows that the samples are predominant fully ordered graphite fields (Figure 4A). The plot of GD versus T (ºC) (Figure 4B) shows the samples aligned with the trend of Ryoke pelites of Wada et al. (1994).

Raman Spectroscopy

The Raman data were obtained in the Technological Center of Nanomaterials (CT nano) at technological park of Belo Horizonte (MG) – BH Tec, using the same methodology proposed in Rantitsch et al. (2016) and the same equipment, a confocal microscope Alpha300R WITEC (Wissenschaftliche Instrumente und Technologie GmbH®, Ulm, Germany) equipped with a Nd-YAG laser with double frequency (2.49 mW, λ = 532.2 nm). Raman spectra were collected with 50× lens objective, where five scans in the 1000–3200 cm^{-1} spectra (first order = 1000–2000 cm^{-1}; second order = 2200–3200 cm^{-1}) were performed with an acquisition time of 30 s. In each sample, five major fields (red,

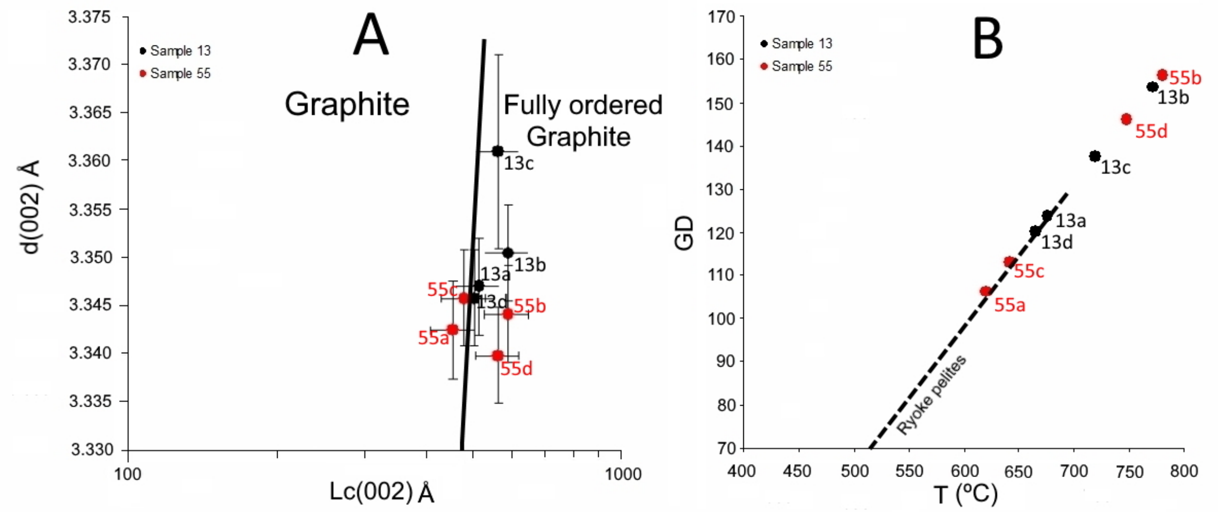

Figure 4 - A - Interplanar spacing $d_{(002)}$ versus crystallite size $Lc_{(002)}$ (Tagiri & Oba, 1986). B - Graphitization degree (GD) versus XRD data temperature compared to the linear relationship for Ryoke pelites of Wada et al. (1994).

green, blue, orange and black) were randomly selected (Figure 5A). Figure 5B shows the analyzed spots (red, green, blue). Figure 5C shows the Raman spectra of these spots. The analysis of the spectra focused on the first-order peaks at~1350 cm^{-1} (D1 band), ~1500 cm^{-1} (D3 band), ~1580 cm^{-1} (G band), and ~1610 cm^{-1} (D2 band) (Figure 5C). The Raman spectroscopy data was evaluated by IFORS method (Lünsdorf & Lünsdorf, 2016).

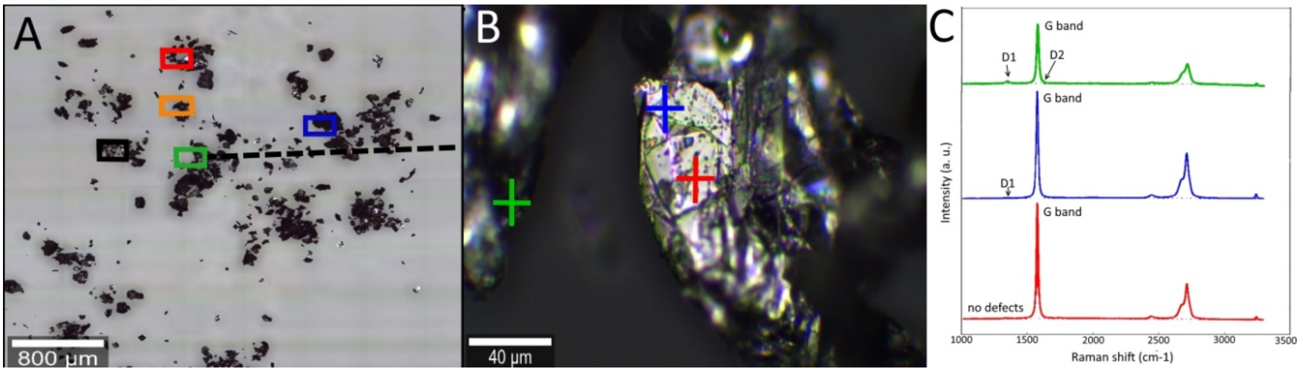

Figure 5 - A - View of a sample in the microscope with five major fields: red; green; orange; blue and black. Photomicrograph taken in PPL. B - Zoom of the blue major field with three spots of analysis red; green; blue. Photomicrograph taken in PPL. C - Raman spectra of the spots.

The IFORS (Interactive Fitting of Raman Spectra) method arose to avoid the process of curve-fitting that is commonly biased by subjectivity, due to many programs requiring manual intervention, especially when baseline manipulation is necessary. It consists of software with an iterative algorithm that does an automated evaluation based on the randomized mutation of function parameters. The approach follows the idea that the Raman spectroscopy of carbonaceous material recorded consists of high-frequency signal components and low-frequency baseline components with added normal distributed noise. The signal components are described by pseudo-Voigt functions and the baseline component by a polynomial, which are modeled simultaneously (Lünsdorf & Lünsdorf, 2016). Table 2 shows the results of Raman spectroscopy, R2 ratio, and the temperature calculations by the IFORS method (Lünsdorf & Lünsdorf, 2016) which revealed temperatures between 542 and 605ºC.

DISCUSSIONS

With the same approach of Rantitsch et al. (2016), which tried to correlate XRD and Raman data, the table 3 shows the mean values of these data. A significant correlation between the d(002) lattice distance and the width of the Raman G band (Figure 6A) and also the R2 ratio (D1/(G + D1 + D2) area ratio of Beyssac et al. (2002a) (Figure 6B) are verified. Metamorphic facies (Beyssac et al., 2002a; Rantitsch et al., 2016) and the semi-graphite/graphite separation (Kwiecińska & Petersen, 2004; Rantitsch et al., 2016) are presented in the figures 6A and 6B.

Table 2 - Raman spectroscopy data of graphite with values obtained by the IFORS method (Lünsdorf & Lünsdorf, 2016).

Sample	D1 ~1350 cm-1						D3 ~1500 cm-1						D2 ~1610 cm-1						G ~1580 cm-1									
	HWHM	sd ±	Center	sd ±	Area	sd ±	HWHM	sd ±	Center	sd ±	Area	sd ±	HWHM	sd±	Center	sd ±	Area	sd ±	HWHM	sd±	Center	sd ±	Area	sd ±	R2	sd ±	T (°C)	sd ±
13-red-p1	21.62	0.00	1348.97	0	107.72	0.19	48.70	0.55	1507.67	0	51.30	0.50	2.97	0.07	1597.41	0	4.23	0.25	8.73	0.00	1580.79	0.00	1481.82	0.65	0.07	0.00	589	37
13-red-p2	21.50	0.01	1350.64	0	168.50	0.26	75.95	0.96	1501.03	0	124.7	2.66	4.71	0.02	1621.51	0	9.51	0.12	8.10	0.00	1580.79	0.00	1625.20	0.42	0.09	0.00	590	37
13-red-p3	20.87	0.02	1348.97	0	213.40	0.90	10.13	0.03	1364.76	0	33.51	0.59	5.90	0.01	1621.51	0	19.40	0.04	8.44	0.00	1580.79	0.00	1990.35	0.41	0.10	0.00	591	37
13-orange-p1	21.50	0.02	1350.64	0	96.43	0.25	22.25	0.15	1501.03	0	21.80	0.48	5.14	0.03	1619.84	0	6.17	0.03	8.10	0.00	1579.96	0.00	1826.03	0.27	0.05	0.00	596	37
13-green-p3	21.58	0.01	1348.14	0	96.64	0.08	-	-	-	-	-	-	-	-	-	-	-	-	8.60	0.01	1579.13	0.00	1806.45	0.50	0.05	0.00	570	37
13-black-p1	20.47	0.05	1348.97	0	23.27	0.31	8.86	0.17	1497.70	0	9.97	0.68	6.08	0.09	1598.24	0	14.06	3.36	7.89	0.01	1580.79	0.00	1817.25	3.97	0.01	0.00	605	37
13-black-p2	25.16	0.10	1351.74	0.5	31.41	0.82	15.35	0.33	1501.03	0	17.58	0.48	1.14	0.01	1594.09	0	1.07	0.04	7.98	0.00	1579.96	0.00	1712.42	0.41	0.02	0.00	603	37
13-black-p3	17.56	0.01	1349.80	0	51.68	0.04	-	-	-	-	-	-	-	-	-	-	-	-	8.89	0.01	1579.96	0.00	1101.39	0.41	0.04	0.00	587	37
13-blue-p1	19.79	0.12	1349.80	0	22.25	0.20	43.33	2.51	1514.88	1.73	51.48	4.31	4.95	0.54	1597.41	0	17.66	5.26	7.86	0.02	1579.96	0.00	1763.54	14.07	0.01	0.00	604	37
13-blue-p2	20.96	0.04	1348.97	0	147.99	1.00	16.48	2.09	1497.15	0.48	18.59	1.26	6.75	0.08	1619.84	0	15.90	0.36	8.79	0.00	1579.13	0.00	2031.21	4.78	0.07	0.00	589	37
13-blue-p3	62.89	3.84	1356.45	0.8	83.12	9.03	56.72	0.25	1506.57	0.48	54.75	1.77	5.69	0.29	1599.71	0	18.37	1.79	8.21	0.03	1580.79	0.00	1844.10	20.11	0.04	0.00	598	37
55- red-p1	25.96	0.01	1334.018	0	185.32	2.12	35.56	3.22	1490.23	4.70	42.39	6.16	11.42	0.94	1592.98	0.96	34.96	1.11	8.13	2.01	1565.01	0.00	1406.35	12.0	0.08	0.00	581	37
55- orange-p1	24.80	0.01	1342.33	0	209.16	0.92	-	-	-	-	-	-	3.74	0.02	1616.52	0	5.56	0.03	8.59	0.02	1574.15	0.00	903.38	2.92	0.19	0.00	576	37
55- orange-p2	45.12	0.10	1323.22	0	242.98	6.33	-	-	-	-	-	-	13.99	0.02	1617.35	0	32.72	0.25	8.02	0.00	1572.48	0.00	929.98	0.29	0.20	0.00	577	37
55- orange-p4	24.27	0.10	1340.67	0	95.70	0.72	-	-	-	-	-	-	50.75	1.01	1598.79	1.27	174.88	44.66	8.89	0.05	1573.31	0.00	445.80	3.61	0.13	0.00	542	37
55- orange-p3	24.06	0.39	1339.00	0	138.57	6.05	-	-	-	-	-	-	23.36	2.53	1603.78	4.80	70.93	63.28	9.74	0.26	1569.99	0.00	659.11	28.46	0.16	0.00	556	37
55- green-p2	-	-	-	-	-	-	-	-	-	-	-	-	-	-	-	-	-	-	8.32	0.01	1568.33	0.00	541.33	0.23	0.00	0.00	563	37
55- green-p3	25.25	0.07	1337.34	0	82.20	0.45	-	-	-	-	-	-	-	-	-	-	-	-	9.25	0.02	1575.53	0.00	475.28	1.17	0.15	0.00	555	37
55- green-p4	23.24	0.01	1339.83	0	266.45	0.09	-	-	-	-	-	-	-	-	-	-	-	-	11.28	0.00	1569.99	0.00	1420.32	0.55	0.16	0.00	555	37
55-black-p2	24.82	0.00	1341.50	0	160.41	0.03	-	-	-	-	-	-	7.95	0.072	1607.38	0	38.10	0.39	8.61	0.00	1569.16	0.00	1840.68	0.69	0.08	0.00	588	37
55-black-p3	26.52	0.07	1334.02	0	48.49	0.16	-	-	-	-	-	-	9.23	4.97	1594.92	5.82	12.10	7.82	6.36	4.12	1568.61	0.00	562.21	485.1	0.05	0.00	593	37
55- blue-p3	25.86	0.01	1340.67	0	262.04	0.48	-	-	-	-	-	-	8.27	0.048	1607.38	0	23.82	0.16	8.64	0.01	1569.99	0.00	1370.07	2.39	0.16	0.00	602	37

sd: standard deviation.

Table 3 - Mean values of the results for XRD and Raman spectroscopy, "n" shows the number of analysis.

	XRD							Raman							
Sample	**n**	**$d_{(002)}$ (Å)**	**sd**	**GD**	**std**	**T(°C)**	**sd**	**n**	**G HWHM (cm^{-1})**	**std**	**R2**	**sd**	**T(°C)**	**sd**
13	4	3.351	0.007	134	15	708	49	11	8.33	0.38	0.05	0.03	593	10
55	4	3.343	0.003	130	25	697	79	11	8.77	1.21	0.12	0.06	572	19

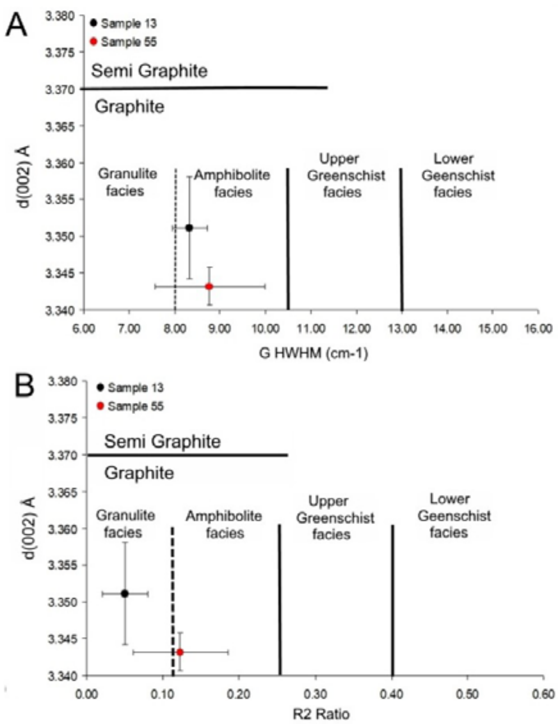

Figure 6 - Graphite samples plotted in diagrams from Rantitsch et al. (2016). A - Half width at half maximum (HWHM) of the G-band versus d(002) lattice distance (Graphite/Semi-graphite at – G HWHM ~ 13.0 and d(002) ~ 3.370). B - R2 ratio (Beyssac et al. 2002a; D1/(G+D1+D2) area ratio) versus d(002) lattice distance (Graphite/Semi-graphite at – R2 ~ 0.4 and d(002) ~ 3.370).

Although G HWHM values (Figure 6A) put all samples in high amphibolite facies, the R2 ratio in figure 6B places the sample 13 in the granulite facies and the sample 55 in the high amphibolites facies. This indicates a good relation of the R2 parameter with the graphite formation temperature, as seen on Beyssac et al. (2002a), Lünsdorf (2015) and Rantitsch et al. (2016). The average data obtained by XRD and Raman spectroscopy in this study are very similar to the data presented by Miranda et al. (2019) for high-grade metamorphic graphite schist in the Itapecerica mines.

By comparing the temperatures (Table 3) obtained from the Raman data (around 583ºC) and XRD data (around 702 ºC), it becomes clear that the temperature obtained by the IFORS method does not correspond to the metamorphism in granulite facies estimated for the region. This is due to the fact that graphite reaches the maximum crystallinity at 600ºC, forming flake-type graphite. According to Beyssac et al. (2002a) and Lünsdorf (2015), around 600°C all graphite becomes fully ordered and the IFORS method cannot calculate higher temperatures. Samples of high-grade metamorphic conditions in Baiju et al. (2005) support an extrapolation of temperatures above 700 ºC on the equation for pelitic rocks of Wada et al. (1994).

The average temperatures found by XRD in this study (table 3), although slightly lower, are similar to the average temperatures (729 ºC) of the high-grade metamorphism samples in Itapecerica mines studied by Miranda et al. (2019).

However, when compared to the metamorphism temperatures around 900 °C described by Coelho & Chaves (2019) in the CSZ, the temperatures around 702 °C found by XRD in this study are much lower. The hypotheses that explain this observation are: the graphitization processes undergone by the CM proceeded with collisional stress until the fully ordered graphite stage, and then the shearing stress in CSZ (Crespo et al., 2006), together with the percolation of metamorphic fluids (represented by quartz veins), changed physically the graphite crystals thus modifying the crystallinity parameters and leading to the relatively low-temperature values found by the technique of XRD.

Or maybe the graphite within the CSZ had modified its crystallinity during decompression promoted by the post-collisional stage making it incompatible with expected for the temperature conditions around 900 °C described by Coelho & Chaves (2019).

From a local geodynamic scenario, the graphite schists and the khondalites of the CSZ, associated with garnet-sillimanite quartzites, banded iron formations and ultramafic rocks, represent the metamorphism of the sediments of a possible Paleoproterozoic oceanic basin. Carvalho et al. (2017) have proposed a tectonic model in which the Archean block is the lower plate and the Mineiro belt is the upper plate that collided at 2.05 Ga, but not included the generation of Itapecerica graphite-rich metasedimentary sequence. Chaves et al. (2015) and Teixeira et al. (2017b) were the first to suggest the possibility of including this sequence in the tectonic discussion.

The paleobasin of CSZ is possibly related to those of the graphite mines of Itapecerica and therefore has undergone a tectonic process analogous to that proposed by Miranda et al. (2019) to the graphite-rich sequences from Itapecerica. According to Miranda et al. (2019) during the pre-collisional stage (2.35–2.08 Ga) the CM-rich sedimentary sequence was deposited on an oceanic basin (Miranda & Chaves, 2021 and references therein). Such sequence was involved during the collision stage (2.07–2.01 Ga) and the CM transformed into graphite under high-grade metamorphism. Figure 7 proposes a tectonic model modified from Carvalho et al. (2017) for the formation of the graphite occurrences within the CSZ around 2.05 Ga, involving the Paleoproterozoic Mineiro orogenic belt.

From a global perspective, the orogenic system highlighted by the CSZ corresponds to the closure of internal oceans and subsequent collision of Archean and Paleoproterozoic crustal blocks that promoted the formation of the supercontinent Columbia (Nuna) (Chaves, 2021 and references therein).

CONCLUSIONS

The Raman spectroscopy and XRD analyses showed data that, on average, are similar to those obtained by Miranda et al. (2019), demonstrating that the graphite at CSZ has high crystallinity. The average temperature found by XRD (702ºC) in this study is close to the high-grade metamorphism samples in Itapecerica mines studied by Miranda et al. (2019). The graphitization processes undergone.

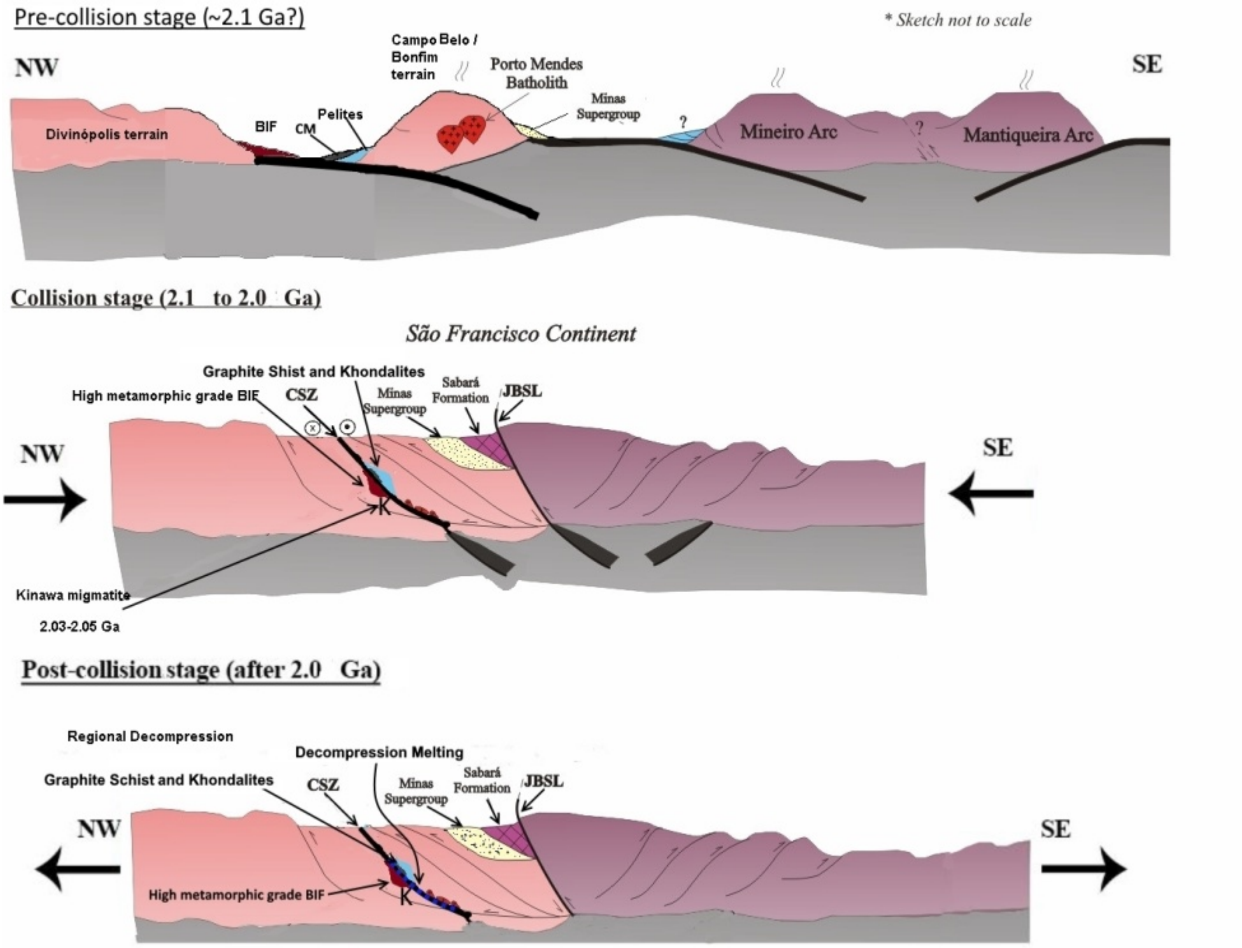

Figure 7 - Geological modeling for the tectonic evolution of CSZ (modified from Carvalho et al., 2017).

CONCLUSIONS

by the CM proceeded with collisional stress until the fully ordered graphite stage, and then the shearing stress in CSZ, together with the percolation of metamorphic fluids (represented by quartz veins), changed physically the graphite crystals thus modifying the crystallinity parameters and leading to the relatively low-temperature values found by the technique of XRD. Or maybe the graphite within the CSZ had modified its crystallinity during decompression promoted by the post-collisional stage making it incompatible with expected for the temperature conditions around 900 °C described by Coelho & Chaves (2019) in the CSZ.

The proximity and the similar geological framework suggest that the precursor basin that formed the graphite occurrences of CSZ is correlated with the precursor basin that originated graphite from Itapecerica. Thus, the source of the CM for the CSZ graphite occurrences possibly is primitive biogenic carbon as Miranda et al. (2019) indicate by the analysis of $\delta^{13}C$ between -21.23 and -27.89 ‰. From a global perspective, the orogenic system highlighted by closure of precursor basins and formation of the CSZ is part of the collisions of Archean and Paleoproterozoic crustal blocks that promoted the formation of the Columbia supercontinent.

ACKNOWLEDGEMENTS

The authors thank FAPEMIG for the financial support (Proc. APQ-00654-16). The second author thanks CNPq for research productivity grant.

REFERENCES

ÁVILA, C.A.; TEIXEIRA, W.; BONGIOLO, E.M.; DUSSIN, I.A.; VIEIRA, T.A.T. Rhyacian evolution of subvolcanic and metasedimentary rocks of the southern segment of the Mineiro belt, São Francisco Craton, Brazil. **Precambrian Research**, v. 243, p. 221–251, 2014. doi:10.1016/j.precamres.2013.12.028.

BAIJU, K.R.; SATISH-KUMAR, M.; KAGI, H.; NAMBIAR, C.G.; RAVINSANKAR, M. Mineralogical characterization of graphite deposits from Thodupuzha-Kanjirappally belt, Madurai granulite block, Southern India. **Gondwana Research**, v. 8, p. 223–230, 2005. doi:10.1016/S1342-937X(05)71120-5.

BARBOSA, N.; TEIXEIRA, W.; ÁVILA, C.A., MONTECINOS, P.M., BONGIOLO, E.M. VASCONCELOS F.F. U-Pb geochronology and coupled Hf-Nd-Sr isotopic-chemical constraints of the Cassiterita Orthogneiss (2.47–2.41-Ga) in the Mineiro belt, São Francisco craton: Geodynamic fingerprints beyond the Archean-Paleoproterozoic Transition. **Precambrian Research**, v. 326, p. 399-416, 2019. ISSN 0301-9268.

BEYSSAC, O.; BOLLINGER, L.; AVOUAC, J.P.; GOFFÉ, B. Thermal metamorphism in the Lesser Himalaya of Nepal determined from Raman spectroscopy of carbonaceous material. **Earth and Planetary Science Letters**,v. 225, p. 233-241, 2004.

BEYSSAC, O.; GOFFÉ, B.; CHOPIN, C.; ROUZAUD, J.N. Raman spectra of carbonaceous material in metasediments: A new geothermometer. **Journal of Metamorphic Geology**, v. 20, n. 9, p. 859-871, 2002a. https://doi.org/10.1046/j.1525-1314.2002.00408.x.

BEYSSAC, O.; ROUZAUD, J.N.; GOFFÉ, B.; BRUNET, F.; CHOPIN, C., Graphitization in a high pressure, low-temperature metamorphic gradient: a Raman microspectroscopy and HRTEM study. **Contributions to Mineralogy and Petrology**, v. 143, p. 19-31, 2002b.

BUSECK, P.R., & BEYSSAC, O. From organic matter to graphite: Graphitization. **Elements**, v. 10, p. 421–426, 2014. doi:10.2113/gselements.10.6.421.

BUSECK, P.R. & BO-JUN, H. Conversion of carbonaceous material to graphite during metamorphism. Geochimimica et Cosmochimica Acta, 49, p. 2003-2016, 1985.

CARVALHO, B.B.; JANASI, V.A.; SAWYER E.W. Evidence for Paleoproterozoic anatexis and crustal reworking of Archean crust in the São Francisco Craton, Brazil: A dating and isotopic study of the Kinawa migmatite. **Precambrian Research**, v. 291, p. 98–118, 2017. doi:10.1016/j.precamres.2017.01.019.

CHAVES, A.O.; GOULART, L.E.A.; COELHO, R.M.; MIRANDA, D.A.; DE OLIVEIRA ARANDA, R.O.; RAMOS, S.L.L.M. High-pressure eclogite facies metamorphism and decompression melting recorded in paleoproterozoic accretionary wedge adjacent to probable ophiolite from Itaguara (southern São Francisco Craton-Brazil). **Journal of South American Earth Sciences,** v. 94, p. 102226, 2019. https://doi.org/10.1016/j.jsames.2019.102226.

CHAVES, A.O. Columbia (Nuna) supercontinent with external subduction girdle and concentric accretionary, collisional and intracontinental orogens permeated by large igneous provinces and rifts: Precambrian Research, 352, 106017, 2021. https://doi.org/10.1016/j.precamres.2020.106017.

CHAVES, A.O. Enxames de diques máficos de Minas Gerais – O estado da arte. **Geonomos**, v. 21, n. 1, p. 29–33, 2013. doi:10.18285/geonomos. v21i1.253.

CHAVES, A.O.; CAMPELLO, M.S.; SOARES, A.C.P. Idade U-Th-PbT de monazitas do sillimanita-cordierita-granada-biotita gnaisse de Itapecerica (MG) e a atuação da orogenia Riaciano-Orosiriana no interior do Cráton São Francisco Meridional. **Geociências**, v. 34, n. 3, p. 324–334, 2015.

COELHO, R.M. & CHAVES, A.O. Pressure-temperature-time path of Paleoproterozoic khondalites from Cláudio shear zone (southern São Francisco craton, Brazil): Links with khondalite belt of the North China craton. **Journal of South American Earth Sciences**, v. 94, 102250, 2019. https://doi.org/ 10.1016/j.jsames.2019.102250.

CRESPO, E.; LUQUE, F.J.; BARRENECHEA, J.F.; RODAS, M. Influence of grinding on graphite crystallinity from experimental and natural data: implications for graphite thermometry and sample preparation. **Mineralogical Magazine**, v. 70, n. 6, p. 697–707, 2006.

DIESSEL, P.R.; BROTHERS, R.N.; BLACK, P.M. Coalification and graphitization in high-pressure schists in New Caledonia. **Contributions to Mineralogy and Petrology**, v. 68, p. 63-78, 1978. doi:10.1016/j.coal.2003.09.003.

FARINA F.A.; ALBERT, C.; LANA, C. The Neoarchean transition between medium and high-K granitoids: Clues from the Southern São Francisco Craton (Brazil). **Precambrian Research**, v. 266, p. 375–394, 2015. doi:10.1016/j.precamres.2015.05.038.

FUCK, R.A.; DANTAS, E.L.; PIMENTEL, M.M.; BOTELHO, N.F.; ARMSTRONG, R.; LAUX, J.H., JUNGES, S.L.; SOARES, J.E.; PRAXEDES, I.F. Paleoproterozoic crust-formation and reworking events in the Tocantins Province, central Brazil: A contribution for Atlantica supercontinent reconstruction. **Precambrian Research**, v. 244, p. 53-74, 2014.

GREW, E.S. Carbonaceous material in some metamorphic rocks of New England and other areas. **Journal of Geology**, v. 82, p. 50-73, 1974.

KLEIN, E.L.; MATOS, D.R.; SANTOS, P.A.D.; CORREA, R.T.; EYBEN, H.S.Z. **Atlas of mineral deposits and selected mineral occurrences of continental Brazil**. CPRM, Brasília, 78 p. 2018.

KWIECIŃSKA, B. Mineralogy of natural graphites. **Polska Akademii Nauk, Prace Mineralogiczne**, 67, p. 5-79. 1980.

KWIECIŃSKA, B. & PETERSEN, H. Graphite, semi-graphite, natural coke, and natural char classification-ICCP system. **International Journal of Coal Geology**, v. 57, p. 99–116, 2004.

LANDIS, C.A. Graphitization of dispersed carbonaceous material in metamorphic rocks. **Contributions to Mineralogy and Petrology**, v. 30, p. 34-45, 1971.

LOPES, S.R.; GONÇALVES, L.; GONÇALVES, C.C. Arcabouço Estrutural, Petrografia e Idades U-Pb em Zircão de Diques Intrusivos em Granitoides da Suíte Lagoa Dourada (2350 Ma) – Cinturão Mineiro, Sudeste do Brasil. **Anuário do Instituto de Geociências,** v. 43, n. 4, p. 66-81, 2020.

LÜNSDORF, N.K. Geothermometry by Raman Spectroscopy of Dispersed Organic Matter [PhD thesis]. **University of Göttingen, Göttingen**, 113 p., 2015.

LÜNSDORF, N.K. & LÜNSDORF, J.O. Evaluating Raman spectra of carbonaceous matter by automated, iterative curve-fitting. **International Journal of Coal Geology**, v. 160-161, p. 51-62, 2016. https://doi.org/10.1016/j.coal.2016.04.008.

MIRANDA, D.A. & CHAVES, A.O. Itapecerica metamafic-ultramafic rocks with E-morb signature: Ophiolitic remnants of the Rhyacian-Orosirian orogeny in southern São Francisco craton?. **Geociências** UNESP, 40, p. 1 – 12, 2021. https://doi.org/10.5016/geociencias.v40i1.15375.

MIRANDA, D.A.; CHAVES, A.O.; CAMPELLO, M.S.; RAMOS, S.L.L.M. Origin and thermometry of graphites from Itapecerica supracrustal succession of the southern São Francisco Craton by C isotopes, X-ray diffraction, and Raman spectroscopy. **International Geology Review**, v. 61, n. 15, p. 1864-1875, 2019. https://doi.org/10.1080/00206814.2018.1564073.

MOREIRA, H., LANA C., NALINI, H.A. The detrital zircon record of an Archaean convergent basin in the Southern São Francisco Craton, Brazil. **Precambrian Research**, v. 275, p. 84–99, 2016. doi:10.1016/j.precamres.2015.12.015.

MOREIRA, H.; STOREY, C.; FOWLER, M.; SEIXAS, L.; DUNLOP, J. Petrogenetic processes at the tipping point of plate tectonics: Hf-O isotope ternary modeling of Earth's last TTG to sanukitoid transition. **Earth and Planetary Science Letters**, v. 551, p. 116558, 2020. https://doi.org/10.1016/ j.epsl.2020. 116558.

NISHIMURA, Y.; COOMBS, D.S.; LANDIS, C.A.; ITAYA, T. Continuous metamorphic gradient documented by graphitization and K-Ar age, southeast Otago, New Zealand. **American Mineralogist**, v. 85, p. 1625-1636, 2000.

NOCE, C.M.; MACHADO, N.; TEIXEIRA, W. U-Pb Geochronology of gneisses and granitoids in the Quadrilatero Ferrıfero (Southern São Francisco Craton): Age constraints for Archean and Paleoproterozoic magmatism and metamorphism. **Revista Brasileira de Geociencias**, v.28, p. 95–102, 1998. doi:10.25249/0375-7536.199895102.

NOCE, C.M.; PEDROSA-SOARES, A.C.; SILVA, L.C.D.; ALKMIM, F.F. O embasamento arqueano e paleoproterozóico do orógeno Araçuaí. **Geonomos**, v. 15, n. 1, p. 17-23, 2007. https://doi.org/10.18285/geonomos.v15i1.104.

OLIVEIRA, A.H. **Evolução Tectônica de um Fragmento do Cráton São Francisco Meridional com base em aspectos estruturais, geoquímicos (rocha total) e geocronológicos (Rb- Sr, Sm-Nd, Ar-Ar, U-Pb)**. Ouro Preto, 92 p., 2004. PhdTesis, Escola de Minas,

PASTERIS, J.D. & WOPENKA, B. Raman spectra of graphite as indicators of degree of metamorphism: **The Canadian Mineralogist**, v. 29, p. 1-9, 1991.

RANTITSCH, G.; LÄMMERER, W.; FISSLTHALER, E.; MITSCHE, S.; KALTENBÖCK, H. On the discrimination of semi-graphite and graphite by Raman spectroscopy. **International Journal of Coal Geology**, v. 159, p. 48–56, 2016. doi:10.1016/j.coal.2016.04.001.

SEIXAS, L.A.R.; BARDINTZEFF, J.M.; STEVENSON, R.; BONIN, B. Petrology of the high-Mg tonalites and dioritic enclaves of the ca.2130 Ma Alto Maranhão suite: Evidence for a major juvenile crustal addition event during the Rhyacian orogenesis, Mineiro Belt, southeast Brazil. **Precambrian Research**, v. 238, p. 18– 41, 2013.

TAGIRI, M. A measurement of the graphitizing degree by the X-ray powder diffractometer. **Journal of Mineralogy, Petrology and Economic Geology**, 76, p. 345–352, 1981.

TAGIRI, M. & OBA, T. Hydrothermal syntheses of graphite from bituminous coal at 0.5–5 kbar water vapor pressure and 300–600°C. **Journal of Mineralogy, Petrology and Economic Geology**, v. 81, p. 260–271, 1986.

TEIXEIRA, W.; ÁVILA, C.A.; DUSSIN, I.A.; CORRÊA NETO, A.V.; BONGIOLO, E.M.; SANTOS J.O.S.; BARBOSA N. Zircon U-Pb-Hf, Nd-Sr constraints and geochemistry of the Resende Costa Orthogneiss and coeval rocks: New clues for a juvenile accretion episode (2.36–2.33 Ga) in the Mineiro belt and its role to the long-lived Minas accretionary orogeny. **Precambrian Research**, v. 256, p. 148–169, 2015. doi:10.1016/j.precamres.2014.11.009.

TEIXEIRA, W.; OLIVEIRA, E.P.; MARQUES, L.S. Nature and evolution of the Archean Crust of the São Francisco Craton, In: HEILBRON, M., CORDANI, U.G., ALKMIM, F.F., (eds): São Francisco Craton, Eastern Brasil. **Regional Geology Reviews, Springer**, p. 29–56, 2017a.

TEIXEIRA, W.; OLIVEIRA, E.P.; PENG, P.; DANTAS, E.L.; HOLLANDA, M.H.B.M. U-Pb geochronology of the 2.0 Ga Itapecerica graphite-rich supracrustal succession in the São Francisco Craton: Tectonic matches with the North China Craton and paleogeographic inferences. **Precambrian Research**, v.293, p. 91–111, 2017b. doi:10.1016/j.precamres.2017.02.021.

USGS, United States Geological Survey. Mineral commodity summaries 2021: U.S. **Geological Survey**, 200 p., 2021. https://doi.org/10.3133/mcs2021

WADA, I.H.; TOMITA, T.; IUCHI, K.; ITO, M.; MORIKIYO, T. Graphitization of carbonaceous matter during metamorphism with reference to carbonate and pelitic rocks of contact and regional metamorphism, Japan. **Contributions to Mineralogy and Petrology**, v. 118, p. 217–228, 1994. doi:10.1007/BF00306643.

WHITNEY, D.L. & EVANS, B.W., Abbreviations for names of rock-forming minerals. **American Mineralogist**, v. 95, n. 1, p. 185–187, 2010. doi:10.2138/am.2010.3371.

WOPENKA, B. & PASTERIS, J.D. Structural characterization of kerogens to granulite-facies graphite: Applicability of Raman microprobe spectroscopy: **American Mineralogist**, v. 78, p. 533-557, 1993.

YOUNG, R.A. Therietveld method. **International Union of Crystallography**: New York, NY, Oxford University Press, 298 p., 1993.

YUI, T.F.; HUANG, E.; XU, J. Raman spectrum of carbonaceous material: a possible metamorphic grade indicator for low-grade metamorphic rocks. **Journal of Metamorphic Geology**, v. 14, p. 115-12, 1996.

Submetido em 5 de julho de 2022
Aceito para publicação em 10 de novembro de 2022